Table V shows the effect on the error range of the predicted reactivity ratios of varying either the sequence distribution, the polymer composition, or the monomer feed while holding the other variables constant. Effects on predicted reactivity ratios of errors of ~9% in the sequence distribution, ~8% in the polymer composition, and ~50% in the monomer feed are shown for a VCl–BMA copolymer. Errors of ~18% in the sequence distribution, ~4% in the polymer composition, and ~1% in the monomer feed are shown for a BD–MMA copolymer. Large errors are not expected in any of the variables, but erroneous reactivity ratios may also arise from a cumulation of smaller errors. The effect on predicted reactivity ratios of an ~2% error in all variables is also shown in Table V for both the VCl–BMA and BD–MMA copolymers. It is doubtful that errors of this degree would occur in all variables simultaneously, but the error range found indicates the experimental care that must be taken in using this approach. Accurate measurement of variables will, however, give favorable reactivity ratio comparisons as shown in Table II.

Conclusions

Reactivity ratios may be predicted in copolymer systems susceptible to sequence distribution measurements by accurately knowing the monomer feed, the copolymer composition, and the copolymer sequence distribution. Reactivity ratios can be obtained with a minimum amount of polymer synthesis and may be used to predict desired copolymer compositions. The single-copolymer reactivity ratio technique could possibly be used to illustrate shifts in reactivity ratios attributed to penultimate effects or polymerization mixture polarity changes.

The single-copolymer reactivity ratio method may prove to be valuable in specific systems where accurate sequence distribution data can be obtained and the use of conventional methods for finding reactivity ratios is not practical.

Acknowledgments. The author would like to acknowledge helpful discussions with Professor H. James Harwood of the University of Akron and the technical assistance of J. E. Simborski of Union Carbide.

Structural Studies of Polyethers $[-(CH_2)_m O-]_n$. VIII. Polyoxacyclobutane Hydrate (Modification I)

Hideto Kakida,[1a] Daisuke Makino, Yozo Chatani, Masamichi Kobayashi, and Hiroyuki Tadokoro[1b]

Department of Polymer Science, Faculty of Science, Osaka University, Toyonaka, Osaka, Japan. *Received March 30, 1970*

ABSTRACT: The structure of crystal modification I of polyoxacyclobutane has been studied by the use of X-ray diffraction and infrared spectroscopic methods. The crystal lattice is monoclinic, $C2/m$-C_{2h}^3, a = 12.3 Å, b = 7.27 Å, c (fiber axis) = 4.80 Å, and β = 91°. Four molecular chains (four monomeric units) and four water molecules are contained in the unit cell, *i.e.*, the crystal is a hydrate. Two polymer chains with essentially planar zigzag structures are joined by a hydrogen-bonded chain of water molecules, resulting in a planar ribbonlike structure. This structure has been corroborated by the normal coordinate treatments carried out on H_2O and D_2O hydrates.

In a previous paper[2] we reported three modifications of polyoxacyclobutane (POCB). The structure determinations of modifications II and III have been described in detail. In this paper we report the structure determination of modification I, the crystal structure of which was found to be a hydrate.

As has been reported in the previous paper, modification II is obtained only as oriented samples and modification III is the most thermally stable form. Figure 1 shows the molecular models of the three modifications. The molecular conformation of modification II is $T_3GT_3\bar{G}$, and that of modification III is $(T_2G_2)_2$. Here G and $\bar{G}$ indicate the right- and left-handed *gauche* forms, respectively. The conformation of modification I is planar zigzag.

(1) (a) Research Laboratory, Mitsubishi Rayon Co. Ltd., Otake, Hiroshima, Japan; (b) to whom correspondence should be addressed.

(2) H. Tadokoro, Y. Takahashi, Y. Chatani, and H. Kakida, *Makromol. Chem.*, 109, 96 (1967).

Experimental Section

Samples. The sample of modification I was prepared by quenching a molten sample in ice water. The uniaxially oriented sample was obtained by stretching the sample in ice water, and the doubly oriented sample was made by rolling the uniaxially oriented sample at a low temperature (about 4°). The deuterated sample was made by steeping the original sample in heavy water for a few days.

Measurements. X-Ray diffraction measurements were made with Ni-filtered Cu Kα radiation. Fiber photographs were taken with cylindrical cameras with radii of 35 and 50 mm. In order to obtain the diffraction spots of higher angles, low-temperature measurements (*ca.* −100°) were also made, giving three times as many reflections as were obtained at room temperature. The intensities of the reflections obtained by the multiple film method were measured by visual comparison with a standard intensity scale.

Japan Spectroscopic Co. DS-402G and Hitachi FIS-1 grating infrared spectrophotometers were used for the infrared absorption measurements. The polarization measurements were made with AgCl and polyethylene polarizers.

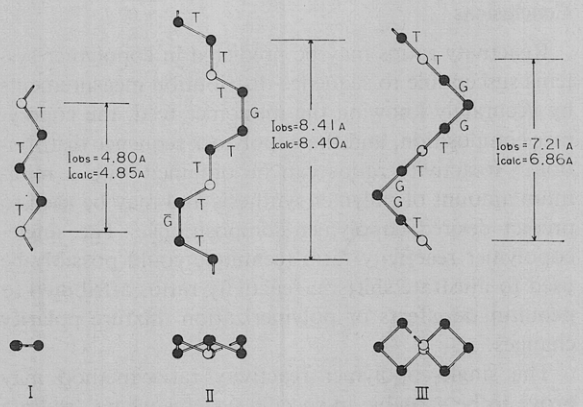

Figure 1. Molecular models of the three modifications of polyoxacyclobutane.[2]

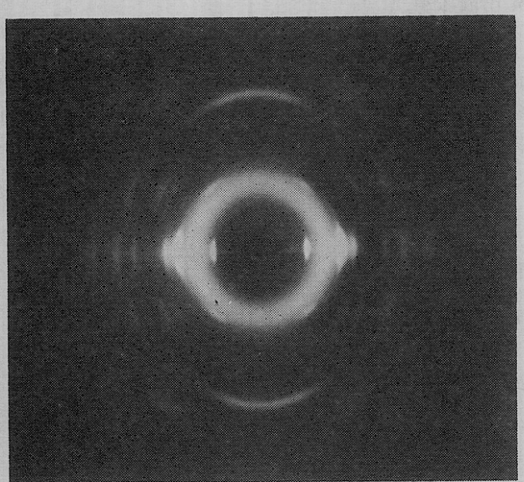

Figure 2. X-Ray fiber photograph of modification I.

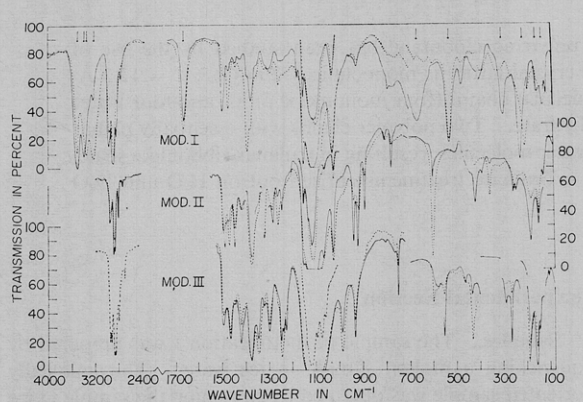

Figure 3. Polarized infared spectra of the three modifications of polyoxacyclobutane: ——, electric vector perpendicular to elongation; - - - - -, electric vector parallel to elongation; · · · · · · · ·, unpolarized data.

Determination of the Structure

The observed fiber identity period of modification I obtained from the X-ray photograph (Figure 2) is 4.80 Å, which is in good agreement with the fiber period of 4.85 Å for a planar zigzag model calculated by assuming the generally accepted bond lengths and bond angles. Thus we have believed that modification I has a planar zigzag structure.

Infrared Absorption Studies. The polarized infrared spectra of modifications I, II, and III are reproduced in Figure 3. The solid and broken curves represent the absorption spectra obtained with the electric vector perpendicular and parallel to the orientation direction, respectively. The bands indicated with arrows in the spectra of modification I are considered to be due to the vibrations of the water molecules, and show very distinct dichroism.

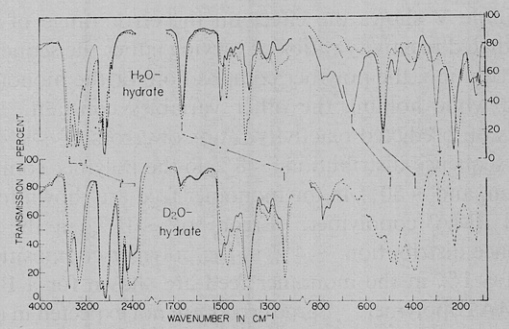

Figure 4. Infrared spectra of modification I: H_2O hydrate (upper part) and D_2O hydrate (lower part).

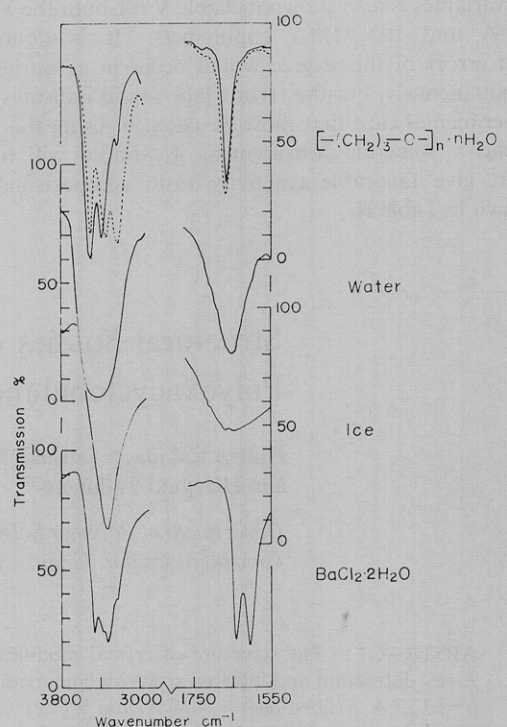

Figure 5. Infrared spectra of the OH stretching and HOH bending vibrations of modification I, water, ice, and barium chloride dihydrate.

These bands, due to the water molecules, could be identified by comparing the normal (upper part) and the deuterated (lower part) spectra shown in Figure 4. The bands indicated with arrows in Figure 3 shift to the longer wavelength side on deuterium substitution, but the remaining bands, which do not, are due to the POCB molecule. Such water bands appear at the OH stretching ($\approx$3300 cm^{-1}), the HOH bending ($\approx$1600 cm^{-1}), and the H_2O libration and translation (below 700 cm^{-1}) regions.

In Figure 5 the spectra in the OH stretching and the HOH bending regions of modification I are compared

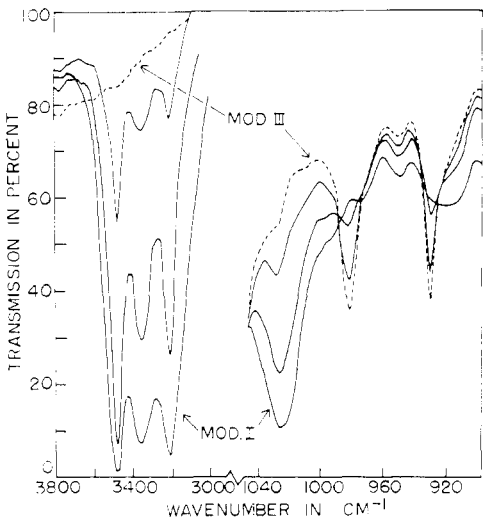

Figure 6. Infrared spectral change on the process of transition from modification I (solid line) to modification III (broken line).

with those of water, ice, and barium chloride dihydrate, $BaCl_2 \cdot 2H_2O$. The OH stretching bands of modification I consist of two perpendicular bands at the higher frequency side, and two parallel bands at the lower frequency side. The HOH bending bands consist of a pair of bands of opposite dichroism with a slightly different frequencies (3 cm^{-1}). The corresponding bands of water and ice are very broad without fine structure. In the spectrum of barium chloride dihydrate, four OH stretching bands and two HOH bending bands were fairly well defined. Thus the bands due to water molecules in modification I are different from those of water and ice, but are quite similar to the bands due to the water of crystallization of barium chloride dihydrate, the salt hydrate.

Figure 6 shows the spectral change in the process of transition from modification I (solid line) to modification III (broken line). For the measurement, a film sample of modification I was held at about $-19°$, and the water was removed continuously by evacuation. With the decrease in intensity of the OH stretching bands, the intensity of the bands due to modification I decrease, and the bands due to modification III appear and increase in intensity. Just when the OH bands disappear, the whole spectrum becomes exclusively that of modification III.

The temperature dependence of the spectral change at atmospheric pressure was also measured. When the temperature of the sample of modification I is raised up to $+10°$, the shape, position, and the dichroism of the bands due to the OH stretching and the HOH bending modes remain unchanged. Heating above $+10°$ results in a similar change in the spectrum as shown in Figure 6, and the water bands disappear completely below the melting point of the polymer. At the same time the polymer transforms into modification III.

Polarized spectra of samples of different degrees of orientation are shown in Figure 7. Spectra (a) are of lower orientation, and spectra (b) are of higher orientation. The water bands show no dichroism in the case of the sample in which the polymer itself has no orientation, and, as is shown in Figure 7, the degree of dichroism of the water bands behaves in the same manner as the polymer bands of modification I.

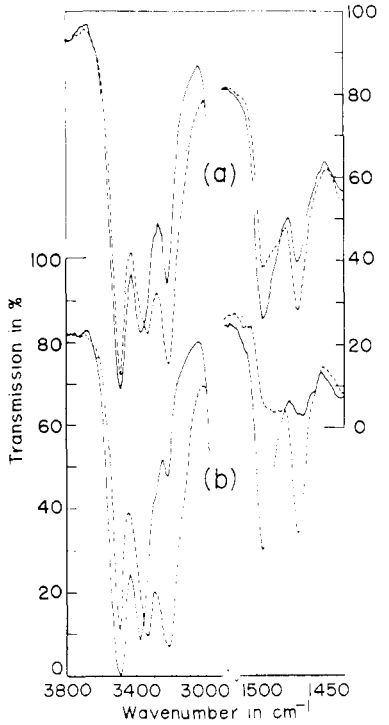

Figure 7. Polarized infrared spectra of modification I of different degrees of orientation: (a) lower orientation, (b) higher orientation.

From these infrared spectroscopic results, we could draw inferences that (1) these water molecules, contained in the sample of modification I, are in the crystalline regions, and (2) the water molecules have definite locations and well-defined orientation in the crystalline regions.

The results of the normal coordinate treatments for the three modifications are reproduced from the previous paper[3] in Figure 8, where the observed frequencies (upper part) and the calculated frequencies (lower part) are schematically shown for the three modifications in the region 1500–80 cm^{-1}. The solid lines, broken lines, and chain lines indicate the perpendicular bands, the parallel bands, and the bands observed with unpolarized light, respectively. The agreement between the observed and calculated frequencies is fairly good. Thus the planar zigzag conformation of modification I is also supported by the infrared studies.

TABLE I
THE ATOMIC COORDINATES OF MODIFICATION I[a]

Atom	x/a	y/b	z/c
O	0.270	0.0	0.250
C_1	0.339	0.0	0.492
C_2	0.265	0.0	0.750
C_3	0.339	0.0	0.008
O_w	0.050	0.0	0.250

[a] The numbering of the atoms is shown in Figure 13. O_w is the oxygen atom of the water molecule.

(3) D. Makino, M. Kobayashi, and H. Tadokoro, *J. Chem. Phys.*, **51**, 3901 (1969).

TABLE II
COMPARISON BETWEEN OBSERVED AND CALCULATED STRUCTURE FACTORS

hkl	$\sqrt{I_o}^a$	$\sqrt{I_c}^b$	*hkl*	$\sqrt{I_o}^a$	$\sqrt{I_c}^b$
2 0 0 1 1 0	60.1	45.2	5 1 1 4 2 1 1 3 1 $\bar{5}$ 1 1 $\bar{4}$ 2 1 $\bar{1}$ 3 1	20.3	23.1
3 1 0 0 2 0	110.4	109.8			
4 0 0 2 2 0	23.7	36.7			
5 1 0 4 2 0 1 3 0	15.1	21.7	6 0 1* 3 3 1* $\bar{6}$ 0 1* $\bar{3}$ 3 1*	8.0	9.2
3 3 0 6 0 0	16.4	28.1	6 2 1* 0 4 1* $\bar{6}$ 2 1*	8.0	6.8
6 2 0 0 4 0	17.9	19.8			
2 4 0 5 3 0 7 1 0	10.4	13.5	7 1 1* 5 3 1* 2 4 1* $\bar{7}$ 1 1* $\bar{5}$ 3 1* $\bar{2}$ 4 1*	13.7	15.7
8 0 0* 4 4 0*	10.9	10.9			
8 2 0* 7 3 0* 1 5 0*		2.2	8 0 1* 4 4 1* $\bar{8}$ 0 1* $\bar{4}$ 4 1*	11.9	11.4
9 1 0* 6 4 0* 3 5 0*	14.2	16.9	8 2 1* 7 3 1* 1 5 1* $\bar{8}$ 2 1* $\bar{7}$ 3 1* $\bar{1}$ 5 1*	9.1	9.1
10 0 0* 5 5 0*	13.7	10.8			
10 2 0* 9 3 0* 8 4 0* 2 6 0* 0 6 0*	16.1	16.7	9 1 1* 6 4 1* 3 5 1* $\bar{9}$ 1 1* $\bar{6}$ 4 1* $\bar{3}$ 5 1*		4.9
11 1 0* 7 5 0* 4 6 0*		3.3	10 0 1* 5 5 1* $\bar{10}$ 0 1* $\bar{5}$ 5 1*	9.7	5.0
12 0 0* 6 6 0* 1 7 0* 10 4 0* 11 3 0*	5.5	6.1	3 1 2 0 2 2 $\bar{3}$ 1 2	8.1	10.8
13 1 0* 8 6 0* 5 7 0*	6.9	4.9	4 0 2 2 2 2 $\bar{4}$ 0 2 $\bar{2}$ 2 2	19.9	18.6
2 0 1 1 1 1 $\bar{2}$ 0 1 $\bar{1}$ 1 1	19.8	17.1			
3 1 1 0 2 1 $\bar{3}$ 1 1	14.5	13.9	4 2 2* 5 1 2* 1 3 2* $\bar{4}$ 2 2* $\bar{5}$ 1 2* $\bar{1}$ 3 2*	28.8	33.0
4 0 1 2 2 1 $\bar{4}$ 0 1 $\bar{2}$ 2 1	19.7	19.7	6 0 2* 3 3 2* $\bar{6}$ 0 2* $\bar{3}$ 3 2*	24.3	17.9

TABLE II (*Continued*)

hkl	$\sqrt{I_o}$[a]	$\sqrt{I_c}$[b]	*hkl*	$\sqrt{I_o}$[a]	$\sqrt{I_c}$[b]
6 2 2* 0 4 2* $\bar{6}$ 2 2*	20.1	22.2	8 2 2* 7 3 2* $\bar{8}$ 2 2* $\bar{7}$ 3 2*		7.3
7 1 2* 5 3 2* 2 4 2* $\bar{7}$ 1 2* $\bar{5}$ 3 2* $\bar{2}$ 4 2*		9.9	1 5 2* $\bar{1}$ 5 2*		6.0
8 0 2* 4 4 2* $\bar{4}$ 4 2* $\bar{8}$ 0 2*	11.6	13.1	9 1 2* 6 4 2* 3 5 2* $\bar{9}$ 1 2* $\bar{6}$ 4 2* $\bar{3}$ 5 2*	24.3	17.1

[a] The observed structure factors $\sqrt{I_o}$'s were put on the same scale as the $\sqrt{I_c}$ ($= \sqrt{mF_c^2}$)'s by setting $\Sigma k\sqrt{I_o} = \Sigma\sqrt{mF_c^2}$, where k is the scale factor and m is the multiplicity. [b] $\sqrt{I_c}$'s of the reflections which overlap on X-ray fiber photographs are $\sqrt{\Sigma mF_c^2}$. * indicates the reflections observed by the low-temperature measurement. The other reflections are the room temperature data.

X-Ray Diffraction Studies. At an early stage of the structural analysis, the reflection spots were indexed with an orthorhombic or a hexagonal cell, except for one set of reflections on the second layer line. Subsequently, a doubly oriented sample was prepared by rolling a uniaxially oriented sample, and this excluded the possibility of a hexagonal cell, because equivalent reflections are not repeated at 60° on the zero layer. By utilizing the data from a doubly oriented sample a monoclinic cell with the following lattice constants was obtained, and whole reflections could be indexed: a = 12.30 Å, b = 7.27 Å, c (fiber axis) = 4.80 Å, and β = 91°. Taking into account the state of the water molecule in the crystal lattice deduced from the infrared studies, we assumed that four monomeric units and four water molecules are contained in the unit cell. The calculated density of 1.17 g/cc is in good agreement with the observed value of 1.11 g/cc. The density measurements of modification I were made by a flotation method by using an aqueous solution of $CaCl_2$ as the flotation medium.

From the systematic absences of the reflections (*hkl*: $h + k \neq 2n$, *h*0*l*: $h \neq 2n$), possible space groups are $C2$-C_2^3, Cm-C_s^3, and $C2/m$-C_{2h}^3. The space group $C2/m$ was confirmed by subsequent refinement of the structure. The crystal structure is shown in Figure 9. The oxygen atoms of water molecules are denoted with w. So far as we know, this is the first case of a hydrate crystal of a synthetic polymer. The atomic coordinates are listed in Table I. The observed and calculated structure factors are compared in Table II. The reflections marked with asterisks are the ones observed at the low-temperature measurements, and the remaining reflections are the room temperature data. The isotropic thermal parameters assumed in the calculations are 15 and 8 Å^2 for the room temperature and low-temperature data, respectively.

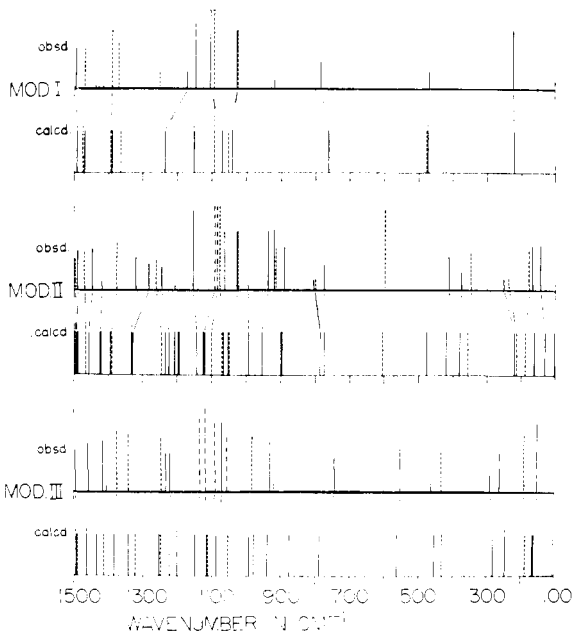

Figure 8. Observed and calculated frequencies for the three modifications of polyoxyacyclobutane in the 1500–80 cm^{-1} region. The solid lines, broken lines, and chain lines represent the perpendicular bands, parallel bands, and the bands observed with unpolarized light, respectively.

Factor Group Analysis and Normal Coordinate Treatment

Factor Group Analysis and Calculation. The symmetry elements of modification I are schematically shown in Figure 10 assuming the positions of the hydrogen atoms of the water molecules. In this ribbon-like structure two chemical units of POCB (two chains) and two water molecules are contained in the fiber identity period. The normal modes may be treated under the factor group isomorphous to the point group C_{2v}.[4] Here the methylene group of the POCB molecule was assumed as a single vibrating unit. According to the results of factor group analysis $13A_1$ modes are

(4) Strictly speaking, because of the monoclinic system of the crystallographic unit cell of modification I (the space group; $C2/m$-C_{2h}^3), the site group of this model is C_s. The vibrations, however, may be reasonably treated under the factor group C_{2v}, since the angle β is 91° (very close to 90°), and the deviation of the molecular symmetry from the exact C_{2v} is negligibly small.

TABLE III
FORCE CONSTANTS

In-plane			
Stretching		Bending	
$K(MM)$	4.30 mdyn/Å	$H(MO_pM)$	0.25 mdyn/Å
$K(MO_p)$	4.60	$H(O_pMM)$	0.25
$K(O_wH_I)$	5.85	$H(MMM)$	0.25
$K(O_wH_{II})$	6.35	$H(H_IO_wH_{II})$	0.685
$K(O_w\cdots H_I)$	0.28	$H_{\parallel}(O_wH_I\cdots O_w)$	0.062 mdyn Å
$K(O_p\cdots H_{II})$	0.18	$H\ (O_wH_{II}\cdots O_p)$	0.062
Repulsive		Stretching-stretching interaction	
$F(MO_pM)$	0.60 mdyn/Å		
$F(O_pMM)$	0.60	$\rho_1[r_1][r_1(+1)]$	−0.33 mdyn/Å
$F(MMM)$	0.60	$\rho_2[r_2][r_2(+1)]$	−0.27
Out-of-plane			
Torsion		Bending	
$F_\tau(MO_p)$	0.11 mdyn Å	$H_\perp(O_wH_I\cdots O_w)$	0.062 mdyn Å
$F_\tau(MM)$	0.13	$H_\perp(O_wH_{II}\cdots O_p)$	0.062
$F_\tau(MMO_pH_{II})$	0.01	$H_\perp(O_wH_I)$	0.01
		$H_\perp(O_wH_{II})$	0.01

infrared active with the parallel polarization, $6B_1$ modes and $13B_2$ modes are infrared active with perpendicular polarization, and $6A_2$ modes are infrared inactive.

The normal mode calculations were made, by means of the mass adjusted cartesian coordinate method, on the ribbonlike structure for both H_2O and D_2O hydrates assuming the methylene group to be a united atom having the mass of the methylene group. The usually accepted molecular parameters were used for the POCB molecule; C–C = 1.54 Å, C–O = 1.43 Å, ∠CCC = ∠CCO = ∠COC = 109°28′. The other molecular parameters were taken from the X-ray data noted

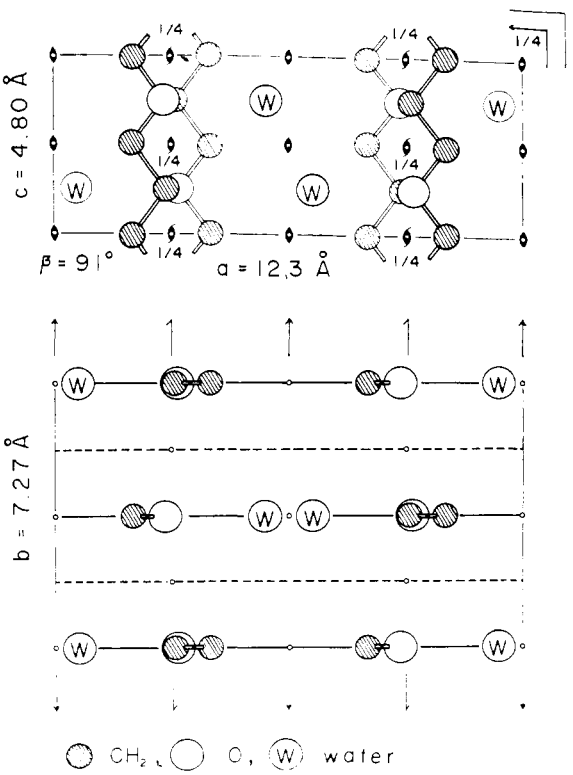

Figure 9. Crystal structure of modification I.

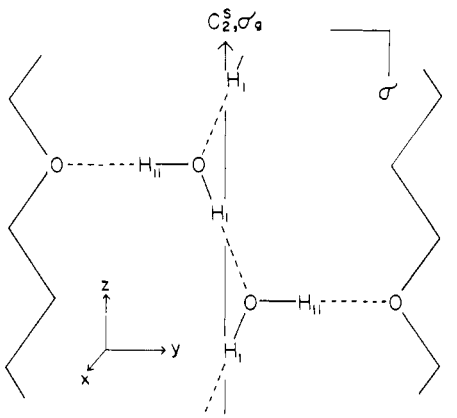

Figure 10. The ribbonlike chain in modification I with its symmetry elements.

before; O(water)...O(polymer) = 2.71 Å, O(water)...O(water) = 2.68 Å. The O–H distance was assumed to be 1.00 Å,[5] and the angle of O–H···O to be 180°.

The internal coordinates used and the numbering of the atoms (groups) are shown in the Appendix (Table V and Figure 13). The usual Urey–Bradley-type force field was used for the POCB molecule. For the field related to the water molecules only the diagonal force constants were used for simplicity. During the process of normal coordinate analysis it was noted that the large separations between the perpendicular and parallel bands of the O–H stretching mode could not be explained by the simple force field mentioned above. When the usual Urey–Bradley-type force field was used, however, it was also difficult to explain the large separations unless the long-range interaction force constants are included. Consequently, we introduced the stretching–stretching interaction force constants between the water molecules, *i.e.*, $\rho_1[r_1][r_1(+1)] = -0.33$ and $\rho_2[r_2][r_2(+1)] = -0.27$ mdyn/Å. The similar long-range interactions have been found for the various molecules linked through the strong hydrogen bonding,

(5) Y. Kyogoku, *Nippon Kagaku Zasshi*, **81**, 1648 (1960).

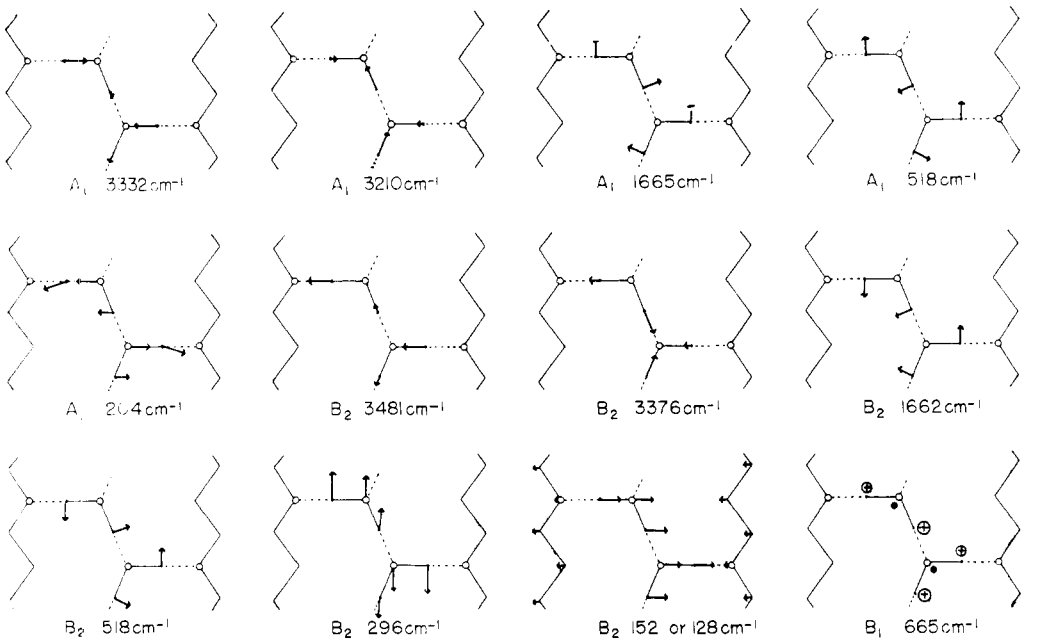

Figure 11. Vibrational modes of modification I H_2O hydrate. The arrow, +, or − represents the displacement of the corresponding atom or group, and its length (or size) is proportional to the L_x-matrix element.

e.g., HCl,[6a] −0.035; HF,[6b] −0.629; $(HCOOH)_2$,[6c] 0.10 and −0.10 mdyn/Å, etc.

The final set of force constants are given in Table III. For D_2O hydrate the same set of force constants was used. The calculated results are shown in Figure 11 and Table IV. In Table IV the observed infrared data, the frequency ratios of H_2O hydrate to D_2O hydrate (ν_H/ν_D), and the potential energy distributions associated with the force constants are also given. In Figure 11 the arrow, +, or −, represents the displacement of the corresponding atom or group for a normal mode, and its length (or size) is proportional to the magnitude of L_x matrix element.

Results of the Normal Coordinate Treatments. Four sharp bands with clear dichroism appearing in the region 3500–3200 cm^{-1} in the H_2O hydrate and 2600–2400 cm^{-1} in the D_2O hydrate are assigned to the stretching vibrations of the O–H (O–D) covalent bonds [ν(OH)]. According to the empirical rule derived by Nakamoto, *et al.*,[7] a shorter length of the O–H···O distance results in a lower frequency of ν(OH), that is, a weaker bonding energy of the O–H bond. In the case of modification I, the O–H···O distance between two water molecules is shorter than that between the oxygen atoms of the water and the polymer. Hence, the value of the stretching force constant of $O–H_{II}$ bond [$O–H_{II}\cdots$O(polymer)] may be regarded as being larger than that of $O–H_I$ bond [$O–H_I\cdots$O(water)]. The calculated results (Figure 11) show that, of the two $A_1(\parallel)$ bands, and of the two $B_2(\perp)$ bands as well, the bands of the higher frequencies are assigned to the vibrational modes in which the contribution of the $O–H_{II}$ stretching is larger than that of the $O–H_I$ stretching, and the reverse is the case for the lower frequency bands.

Two bands observed at 1665(∥) and 1662(⊥) cm^{-1} in the spectrum of H_2O hydrate shift to 1215 cm^{-1} on deuterium substitution, and are assigned to the HOH bending modes of water molecule [δ(HOH)] belonging to the A_1 and B_2 species, respectively, as shown in Figure 11. In the spectrum of D_2O hydrate the frequency splitting of 1215 cm^{-1} [δ(DOD)] band is not clearly detected.

In the spectrum of H_2O hydrate two strong bands are found at 665 and 518 cm^{-1}, and a weak band at 469 cm^{-1}. The weak band is also found in D_2O hydrate at the same position, and has been assigned to the skeletal bending mode of the POCB molecule.[8] The remaining two bands shift to longer wavelength side (496 and 371 cm^{-1}) by deuterium substitution. Taking their positions and the magnitudes of the frequency shifts into account, we may consider that they are attributed to the librational modes of the water molecules.

A rigid body water molecule in a crystal field has three types of librational modes around the three principal axes of inertia, namely, a wagging mode [$w(H_2O)$], a twisting mode [$t(H_2O)$], and a rocking mode [$r(H_2O)$]. In the case of modification I, the four almost pure librational modes belonging to $A_1[r(H_2O)]$, $B_1[w(H_2O), t(H_2O)]$, and $B_2[r(H_2O)]$ species are expected to be observed in the infrared spectrum from the normal coordinate calculation. It may be reasonable to regard the intensity of the $t(H_2O)$ mode as being very weak compared with the other two modes. Actually, $t(H_2O)$ of some hydrates ($CrCl_3\cdot 6H_2O$, $MgSO_4\cdot 7H_2O$, etc.), which are observable in the neutron inelastic scattering method,[8] cannot be observed in the infrared spectra.[9] Consequently, three librational modes of

(6) (a) D. F. Hornig and W. E. Osberg, *J. Chem. Phys.*, **23**, 662 (1955); (b) J. S. Kittelsberger and D. F. Hornig, *ibid.*, **26**, 637 (1967); (c) S. Kishida and K. Nakamoto, *ibid.*, **41**, 1558 (1964).

(7) K. Nakamoto, M. Morgoshes, and R. E. Rundle, *J. Amer. Chem. Soc.*, **77**, 6480 (1955).

(8) H. J. Prask and H. Boutin, *J. Chem. Phys.*, **45**, 3284 (1966).

(9) I. Nakagawa and T. Shimanouchi, *Spectrochim. Acta*, **20**, 429 (1964).

TABLE IV
NORMAL VIBRATIONS OF MODIFICATION I OF POLYOXACYCLOBUTANE[a]

Species	H_2O hydrate, cm^{-1} Obsd[b]	H_2O hydrate, cm^{-1} Calcd	D_2O hydrate, cm^{-1} Obsd[b]	D_2O hydrate, cm^{-1} Calcd	(ν_H/ν_D)[c] Obsd	(ν_H/ν_D)[c] Calcd	Assignments[d] and the potential energy distribution[e] in force constants
	3332(∥) vs	3353	2460(∥) vs	2453	1.35	1.37	$\nu(OH_{II})$; $K(O_wH_{II})$ (95)
	3210(∥) vs	3212	2397(∥) vs	2323	1.34	1.38	$\nu(OH_I)$; $K(O_wH_I)$ (93)
	1665(∥) s	1666	1215(∥) s	1217	1.37	1.37	$\delta(HOH)$; $H(H_IO_wH_{II})$ (90)
A_1	518(∥) vs	516	371(···) vs	365	1.40	1.41	$r(H_2O)$; $H_{\parallel}(O_wH_{II}\cdots O_p)$ (50), $H_{\parallel}(O_wH_I\cdots O_w)$ (49)
		469		469		1.00	δ(POCB skeleton)
		468		469		1.00	
	204(∥) m	202	202(···) m	194	1.01	1.04	$T_y(H_2O)$; $K(O_p\cdots H_{II})$ (45), $K(O_w\cdots H_I)$ (42)
		53		53		1.00	T_y(POCB), $T_{yz}(H_2O)$
		31		30		1.03	$T_z(H_2O)$, $-T_z$(POCB)
	3481(⊥) vs	3501	2587(⊥) vs	2565	1.35	1.36	$\nu(OH_{II})$; $K(O_wH_{II})$ (82), $K(O_wH_I)$ (11)
	3376(⊥) vs	3374	2499(⊥) s	2429	1.35	1.39	$\nu(OH_I)$; $K(O_wH_I)$ (79), $K(O_wH_{II})$ (11)
	1662(⊥) s	1669	1215(⊥) s	1222	1.37	1.37	$\delta(HOH)$; $H(H_IO_wH_{II})$ (90)
B_1	518(⊥) vs	524	371(···) vs	378	1.40	1.39	$r(H_2O)$; $H_{\parallel}(O_wH_I\cdots O_w)$ (50), $H_{\parallel}(O_wH_{II}\cdots O_p)$ (43)
	469(⊥) w	469	469(···) m	469	1.00	1.00	δ(POCB skeleton)
		468		469		1.00	
	296(⊥) m	297	286(···) m	280	1.03	1.06	$T_z(H_2O)$; $K(O_w\cdots H_I)$ (92)
	152(⊥) w	144	152(···) m	138	1.00	1.04	$T_y(H_2O)$, $-T_y$(POCB); $K(O_p\cdots H_{II})$ (93)
	128(⊥) w		128(···) m		1.00		
		16		16		1.00	T_z(POCB)
	665(⊥) s	662	497(···) m	489	1.34	1.35	$w(H_2O)$; $H_{\perp}(O_wH_I\cdots O_w)$ (48), $H_{\perp}(O_wH_{II})$ (19), $H_{\perp}(O_wH_{II}\cdots O_p)$ (18), $H_{\perp}(O_wH_I)$ (14)
B_2		529		377		1.40	$t(H_2O)$; $H_{\perp}(O_wH_{II}\cdots O_p)$ (44), $H_{\perp}(O_wH_I\cdots O_w)$ (26)
	223(⊥) m	249	223(···) m	249	1.00	1.00	τ(POCB skeleton)
		236		235		1.00	
		81		80		1.01	$\tau(H_2O$, POCB skeleton)
		12		11		1.09	$T_x(H_2O)$, $-T_x$(POCB)

[a] The skeletal stretching vibrations of the POCB molecule are omitted. [b] vs, very strong; s, strong; m, medium; w, weak. [c] The frequency ratios of H_2O hydrate to D_2O hydrate. [d] The vibrational modes are deduced from Figure 11: ν, stretching; δ, bending; r, rocking; w, wagging; t, twisting; τ, torsion; T, translation. [e] The potential energy distributions were omitted for the vibrations of the POCB molecule and the unobserved vibrations of low frequencies.

modification I are expected to give rise to the absorptions with appreciable intensity.

In the course of the calculations it has been found that, by using a suitable set of the force constants, the frequency separation between the A_1 and B_2 species of the $r(H_2O)$ mode is about 8 cm^{-1}. This result supports the observed data that the dichroism of the 518 cm^{-1} band is poor compared with the other water bands, or in other words this band is composed of two components of different dichroism. The parallel component of the 518-cm^{-1} band will be undoubtedly assigned to the rocking mode of the H_2O molecule belonging to the A_1 species from its dichroism. Thus, we may reasonably assign the perpendicular component of the 518-cm^{-1} band to the $r(H_2O)$ mode of the B_2 species, and therefore the 665-cm^{-1} band to $B_1[w(H_2O)]$.

On deuterium substitution, the 665- (B_1) and 518- (A_1 and B_2) cm^{-1} bands of the H_2O hydrate shift to 497 and 371 cm^{-1}, respectively. The ratios of their frequencies (ν_H/ν_D), 1.34 and 1.40, are in good agreement with the calculated values, which are 1.35 (B_1) and [1.41 (A_1) and 1.39 (B_2)], respectively.

Five distinct absorption bands are observed in the 400–100-cm^{-1} region of the spectrum. A strong perpendicular band at 223 cm^{-1} shows no frequency shift on deuterium substitution, and could be assigned

to the skeletal torsional mode of the POCB polymer as reported in the preceding paper.[3] Only one torsional band belonging to the B_2 species of the single chain factor group is expected for the isolated POCB chain, which has C_{2v} symmetry. On the other hand, though a few bands due to the torsional vibrations should be expected in the present treatment because of the C_s site symmetry of the polymer chain itself, the inactive bands in the single chain treatment are expected to be very weak in intensity. Therefore, the remaining four bands may be reasonably considered to be associated with the water molecules.

The 296($\perp$)- and 204($\parallel$)-cm^{-1} bands shift to lower frequency (286 and 202 cm^{-1}) on deuterium substitution. From the normal coordinate treatment, these bands are assigned to the in-plane pure translational modes of the H_2O molecules including few contributions of the intrachain modes of the polymer molecule as shown in Figure 11. The observed frequency ratios of the 296- and 204-cm^{-1} bands to the corresponding bands of the deuterated crystal are 1.03 and 1.01, respectively, in good agreement with the calculated values, 1.06 and 1.04, respectively.

The remaining two weak bands at 152 and 128 cm^{-1} show perpendicular dichroism, and are assignable to the B_1 or B_2 modes. Though it is difficult to determine their assignments from the results of the present normal coordinate treatment only, one of these would be assigned to the B_2 mode (see Figure 11).

Discussion

The distances between the oxygen atoms determined by X-ray analysis (water–water, 2.68 Å; water–polymer, 2.71 Å) are shorter than twice the van der Waals radius of an oxygen atom, 2.80 Å, as shown in Figure 12. This fact suggests the presence of hydrogen bonds both from water to water and from water to POCB molecules. The presence of hydrogen bonds is also supported by the infrared studies discussed below.

The OH stretching [ν(OH)] and the HOH bending [δ(HOH)] vibrations of the water molecules of modification I show distinct dichroism at 3480–3200 and $\approx$1660 cm^{-1}, respectively. The frequencies of the OH stretching vibrations of modification I are comparable to those of some substances having hydrogen-bonded water molecules, such as ice[7] or oxalic acid dihydrate, $(COOH)_2 \cdot 2H_2O$.[7]

The free water molecule, which has C_{2v} symmetry, has only three intramolecular vibrations (ν_1, ν_2, and ν_3) which are infrared active. However, water molecules bound in the crystal have intramolecular vibrations as well as rotational and translational modes which are potentially infrared active. Actually, in a number of substances having hydrogen-bonded water molecules, distinct infrared absorption bands[5,9,10] or neutron inelastic scattering data[8,11] are observed due to the rotational or translational vibrations of the water molecule. In the case of POCB modification I several infrared bands also appear below 700 cm^{-1}, which are assignable to the librational or translational modes of

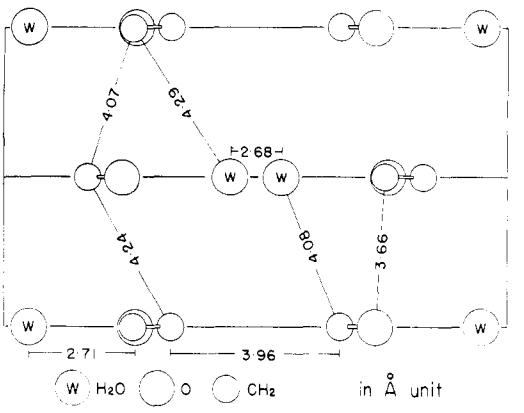

Figure 12. The interatomic distances of modification I.

the water molecule. This indicates the existence of forces which bind water molecules into the modification I crystal.

The oxygen atom of a water molecule in ice contributes two hydrogen bonds, resulting in four bonds (including two OH covalent bonds) arranged tetrahedrally. In the case of POCB modification I (see Figure 13), the O···O distances between neighboring molecular sheets parallel to the *ac* plane are longer than 4 Å. These O···O distances are far longer than the distance of the van der Waals radii of oxygen atoms, 2.80 Å, and there is no possibility of forming hydrogen bonds between the sheets. Thus it may be concluded that the oxygen atom of the water molecule forms one hydrogen bond with the neighboring water molecule in the same plane, giving a hydrogen bonded two-dimensional sheet structure. The molecular arrangement of one layer parallel to the *ac* plane is schematically shown in Figure 10.

The state of the water molecules in this compound has been investigated from the thermodynamic viewpoint by Yoshida, Sakiyama, and Seki[12] in a parallel study. Dehydration isotherms exhibit a stepwise change in vapor pressure with the amount of water dehydrated, a typical feature of stoichiometric water of hydration. At the same time they measured the temperature dependence of dehydration pressure, and evaluated the heat of dissociation of the water molecule to be 13.6 kcal/mol.

The stretching force constants [K(O···H)] of the hydrogen bonds from water to water and from water to polymer of modification I were calculated to be 0.28 and 0.18 mdyn/Å, respectively. These values are comparable with those obtained for $(HCOOH)_2$ (0.36 mdyn/Å)[6c] or ice (0.15 mdyn/Å),[5] suggesting that the strength of the hydrogen bonds of modification I is comparable in magnitude to that in $(HCOOH)_2$ or ice. Here it is of interest to compare the ratio of the values of K(OH) to K(O···H) with that of the bond energy of O–H bond (E) to the dissociation energy of O···H bond (D). The ratio of $K(OH_I)/K(O\cdots H_I) = 1:0.05$, and $K(OH_{II})/K(O\cdots H_{II}) = 1:0.03$. Though the dissociation energy, 13.6 kcal/mol, is the sum of the two unequivalent hydrogen bonds ($O_w\cdots H_I$ and

(10) J. Van Der Elsken and D. W. Robinson, *Spectrochem. Acta*, **17**, 1249 (1961).
(11) H. Boutin, G. J. Safford, and H. R. Danner, *J. Chem. Phys.*, **40**, 2670 (1964).
(12) S. Yoshida, M. Sakiyama, and S. Seki, *Rep. Progr. Polym. Phys. Jap.*, **12**, 245 (1969).

TABLE V
INTERNAL COORDINATES

In-plane coordinates
Bond lengths
$R_1[O_p\text{–}M_1]$, $R_2[M_1\text{–}M_2]$, $R_3[M_2\text{–}M_3(+1)]$, $R_4[M_3\text{–}O_p]$, $r_1[O_w\text{–}H_I]$, $r_2[O_w\text{–}H_{II}]$, $h_1[O_w(-1)\text{–}H_I]$, $h_2[O_p\text{–}H_{II}]$
Bond angles
$\Theta_1[\angle M_3O_pM_1]$, $\Theta_2[\angle O_pM_1M_2]$, $\Theta_3[\angle M_1M_2M_3(+1)]$, $\Theta_4[\angle M_2(-1)M_3O_p]$, $\phi[\angle H_IO_wH_{II}]$, $\theta_1[\angle O_w(-1)H_IO_w]$, $\theta_2[\angle O_wH_{II}O_p]$.

Out-of-plane coordinates
Bond angles
$\chi_1[\angle O_w(-1)H_IO_w]$, $\chi_2[\angle O_wH_{II}O_p]$, $\pi_1[\angle O_wH_I]$, $\pi_2[\angle O_wH_{II}]$
Internal rotation angles
$\tau_1[\angle M_3O_pM_1M_2]$, $\tau_2[\angle O_pM_1M_2M_3(+1)]$, $\tau_3[\angle M_1M_2M_3(+1)O_p(+1)]$, $\tau_4[\angle M_2(-1)M_3O_pM_1]$, $\psi_1[\angle M_2(-1)M_3O_pH_{II}]$, $\psi_2[\angle M_2M_1O_pH_{II}]$.

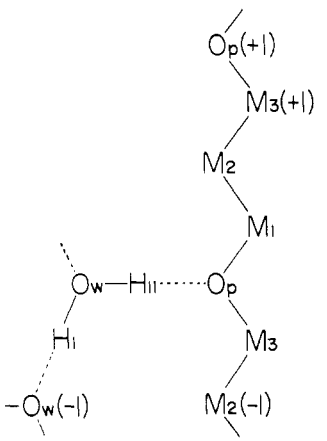

Figure 13. The numbering of the atoms (groups) for modification I.

$O_p\cdots H_{II}$), the ratio of E/D, the average value for the two hydrogen bonds, is calculated to be 1:0.06 by using the value of bond energy of the O–H bond (Coulson),[18] 119.5 kcal/mol. Thus the values obtained from spectroscopic methods are in the same order of magnitude as the one obtained from thermodynamical method.

Finally we may naturally ask if it is necessary for the water molecules to be in the crystal lattice of modification I as water of crystallization. The molecular structure of modification I is planar zigzag, and this conformation itself is considered to be more unstable than that of modifications II or III because of the parallel alignment of the dipole moments at the COC group. Therefore there must be stabilizing forces in the planar zigzag conformation of the polymer molecule. Since modification I is stable only in the presence of water, we conclude that the water molecules may contribute to stabilization of the planar zigzag conformation by forming a hydrogen-bonded network not only between the water molecules but also between the water molecules and polymer chains.

Appendix

The internal coordinates used are given in Table V, and the numbering of the atoms or groups is shown in Figure 13.

(13) C. A. Coulson, "Valence," Claredon Press, London, 1953.